

FURTHER STUDIES OF COLLECTIVE ACCELERATION OF POSITIVE PARTICLES USING INTENSE ELECTRON BEAMS

B. Ecker and S. Putnam
Physics International Company, San Leandro, CA., 94577
and
D. Drickey, Department of Physics, UCLA

Protons at 12 MeV and nitrogen nuclei (N^{+7}) at 29 MeV were produced during propagation of a pulsed 100 kA, 1 MV electron beam (peak values) through initially neutral hydrogen and nitrogen, respectively. Applied longitudinal magnetic fields of 250 gauss or more severely suppressed proton acceleration; 100 gauss had no effect. Protons having at least 3 MeV were observed 11 cm from the plane of injection of the electron beam into the gas-filled acceleration region. At the time of acceleration, the electron beam current front had already propagated substantially beyond the acceleration region. Use of a colder beam than in a previous study¹ resulted in increased particle energy and in greater sensitivity of proton energy to hydrogen density. The localized pinch model is strongly supported by some of the data and is compatible with all results.

Introduction

The first observation of ions accelerated by intense electron beams propagating through initially neutral gas was in 1970 by Graybill and Uglum.² Since then a number of experimental studies have been reported,^{1,3-6} four theoretical models have been put forth to explain the data,⁷⁻¹² and three review papers have been presented.¹³⁻¹⁵ The present study was a small program that aimed at bringing us closer to a definite conclusion about the nature of the acceleration process and its cut-off mechanisms. To this end we have investigated mainly the effects of electron beam temperature and of an applied longitudinal magnetic field, and the spatial and temporal relationship between the electron beam and the accelerated ion bunch. As pointed out by Yonas,¹⁵ of the four theoretical models thus far proposed only the localized pinch model (LPM)^{11,12,20} runs into no harsh discrepancies with experimental data. Results presented here, while not conclusive, give new support to the LPM viewpoint.

Apparatus and Procedures

Figure 1 shows the apparatus used. The diode of the electron beam generator (Physics International 738 Pulserad) was a 2.0 inch diameter, smooth, flat cathode of conductive epoxy and a transmission anode of 0.25 mil aluminized Mylar. The anode-cathode gap was 3/8 in. The electron beam current increased at the rate of 7.5×10^{12} A/sec for 10 nsec, reached peak value of 115 kA at $t=35$ nsec, and decreased to zero at $t=100$ nsec. Diode voltage increased to 1.0 MV by $t=15$ nsec, lingered around 0.85 MeV for 30 nsec, and decreased to zero at $t=90$ nsec.

The acceleration chamber was a 3-in. diameter copper tube, extending from the anode ($z=0$) to $z=73$ cm. Four Rogowski coils to measure local time-of-arrival of the electron beam current were in the copper tube at $z=1$,

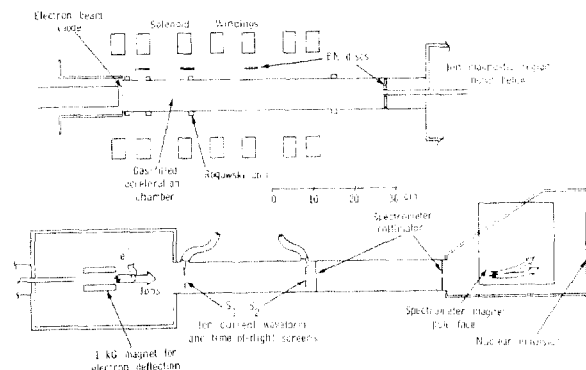


Fig. 1 Experimental set-up for collective linear acceleration and diagnosis of ions.

6.35, 16.5, and 50 cm. A 1.1 cm diameter on-axis tube, 20 cm long, provided a path for particles to pass to the ion diagnostics region. Electrons that traversed this tube were stripped away from the higher momentum positive particles by space charge forces and by a 1 kg magnet with 3 inch poleface diameter. Two copper screens with on-axis holes acted as particle current collectors (much as a Faraday cup) and measured both ion time-of-flight (TOF) and ion current waveform. The first screen was at $z=108.6$ cm and the second was 28.9 cm behind the first. Figure 2 shows typical signals from the screens for protons accelerated to 4.7 MeV. On-axis particles passed through a collimator system (two 0.32 cm holes, 30.5 cm apart, the first at $z=140$ cm) and into a magnetic spectrometer using nuclear emulsions. The velocity from TOF, the ion range, and the momentum per charge together gave a complete determination of particle type, charge state, and energy.

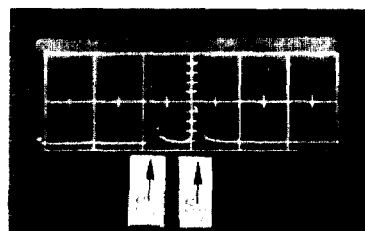


Fig. 2 Proton waveforms at 4.7 MeV from current collector/TOF screens. The two signals were electronically added with an extra delay of 8.95 nsec in the cable from S_2 . Time scale is 21.7 nsec per large division. S_1 (S_2) is 1.4 (0.7) ampere/large division.

A 49 cm long, independently pulsed solenoid was placed around the copper tube

with one end at $z=0$ in order to study ion acceleration in a longitudinal magnetic field. The magnetic field had a 40 msec period and was radially uniform to within 2% in $r \leq 3$ cm and longitudinally uniform (in $r \leq 3$ cm) within 10% over the physical length of the solenoid (measured inside the 3-inch copper acceleration chamber). The field applied at the time of beam injection was oscilloscope-monitored on all shots by measuring the slow solenoid current waveform with a resistive shunt and electronically adding the very fast diode current waveform from a magnetic probe.

Results

A. Pressure Dependence of Proton Acceleration: Effects of Electron Beam Temperature

Using an electron beam with current and voltage waveforms very similar to those of the present study, Rander, et al.¹ found that the peak proton energy of 1-2 MeV varied little with pressure. Our new results (Fig. 3) show a marked dependence of proton energy on hydrogen pressure, and the highest proton energy attained, 12.2 MeV, is 6 times higher than that found previously.

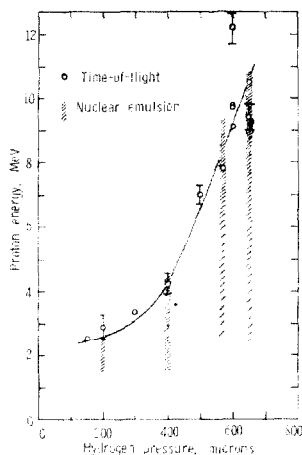


Fig. 3
Final energy of accelerated protons versus hydrogen pressure.

The major difference between the two experiments was in the cathode of the beam-accelerating diode. Rander used a 3-inch diameter, 600-needle cathode; a 2-inch diameter smooth cathode was used in the experiments reported here. The work of Bradley, et al.¹⁶ has shown that such a change in cathode surface structure results in substantial decreases in beam temperature. For this reason we correlate the new proton energy versus pressure data with a decrease in electron beam temperature.

No accelerated protons were detected from three pulses into hydrogen at 800 μ . (The low-energy limit of detection of the magnetic spectrometer was 0.65 MeV for protons.) The proton momentum spread, $\Delta p/p_{\text{max}}$, increased from 0.15 to 0.5 as pressure increased from 200 μ to 650 μ hydrogen. The propagation velocity of the electron beam also increased with pressure, with the greatest increase found in going from 650 μ to 800 μ hydrogen (Fig. 5, discussed below).

B. Location of Acceleration Region, Acceleration Field Strength, and Total Proton Flux.

Boron nitride (BN) discs were used to detect and measure a radial flux of protons, utilizing the reaction



The proton energy threshold for this reaction is 3 MeV and the final decay has a 20.5 min. half-life. Positron counting rates using a high-efficiency sodium iodide counter verified the half-life and were the data from which proton flux was calculated. On one pulse in 600 μ hydrogen, BN discs were placed outside holes in the chamber at $z=5$, 11, and 27 cm. On a second pulse at the same pressure two discs were inside the chamber at $z=63$ cm, facing the anode with center 1 inch off-axis. These two discs indicated the largest proton flux of the five measurements, 10^{10} - 10^{11} protons/cm². The three discs at radial positions showed that radial flux was present and increased away from the anode. Radial flux at $z=5$ cm was too low to detect. Several deductions can be made from the data: (a) Protons with energy at least 3 MeV were observed to emerge from the hole 11 cm from the anode.

(On that pulse, the proton energy determined with the ion diagnostics was 9.1 MeV.) This data confirms that the acceleration begins in the immediate vicinity of the anode, as inferred earlier,^{1,2} and it implies a firm lower limit on the accelerating field of 0.3 MeV/cm. This value is clearly the most pessimistic evaluation of these data; 1 MeV/cm is not at all an unreasonable inference. (b) One explanation for the detection of a radial flux of protons is the following. Even if the protons initially had purely paraxial velocities, the radially outward force resulting from interaction with the electron beam's azimuthal magnetic field could explain the observed appearance of protons at the chamber walls if the radial electrostatic field around the ion bunch diminished with distance from the anode. (c) Having measured local flux at the chamber walls and end-plate, the total number of accelerated protons can be estimated, giving $(0.5 \text{ to } 2) \times 10^{12}$ protons per pulse at 600 μ hydrogen. The BN flux measurements were not made at lower pressures where proton current waveforms showed about an order of magnitude increase in flux on some pulses. These flux determinations are in agreement with previous results.^{1,2}

C. Nitrogen Ion Acceleration

The electron beam was injected into nitrogen at several pressures in the range 20 μ to 150 μ . At the extremum pressures of 20 μ and 150 μ no ion signals were obtained with the TOF screens; nuclear emulsions were not used on these pulses so we only know that the ion current was below the screen detection threshold of 0.07 ampere.

One pulse into nitrogen at 80 μ was diagnosed with both TOF screen and nuclear emulsions. Emulsion tracks due to N^{+6} and N^{+7} at 29.3 ± 2.2 MeV and protons at 3.85 ± 0.35 MeV were found. The presence of protons,

probably due to outgassing of water vapor or hydrogen, makes possible a comparison of particle energy per charge Z over a wide range of charge, in this case from $Z=1$ to $Z=7$. The N^{+7} and proton energies just given are in ratio 7.7 ± 1.3 . Within experimental error, the energy per charge is constant, in agreement with previous results.^{2,6} The energy of the N^{+6} ions was indistinguishable from that of the N^{+7} ions (though the difference in momentum per charge was easily resolved), suggesting charge exchange in the nitrogen gas enroute to the spectrometer.

One pulse into nitrogen at 40μ , again with both TOF and emulsions, gave different results. Nitrogen ions with charge $+4$ through $+7$ were observed; protons were not observed; and energy per charge was not constant among the different charge states present. N^{+6} at 27 ± 0.5 MeV was the most energetic particle detected from this pulse.

D. Effects of Applied Longitudinal Magnetic Field.

The azimuthal magnetic self-field at the edge of a 50 kA beam (typical net current measurement from Rogowski coil) of 2 inch diameter is about 4 kG; considering that the beam pinches, values much higher than this are more realistic. On this scale of reference, the effects of both small and large longitudinal magnetic fields were studied. Briefly, 100 G had no effect while 250 G, 500 G, 3 kG, and 10 kG fields eliminated proton acceleration on all pulses but one. This exception, one of the two 500 G pulses, is interesting because proton energy was the same as when no field was applied (≈ 3 MeV), but the flux was 2-3 orders of magnitude lower.

E. Location and Motion of Particle Bunch Relative to Electron Beam.

The Rogowski coil signals were used to examine the location of the electron beam current front as a function of time. The beam had $v/(\gamma-1) > 1$, so the propagation velocity of the beam front was considerably less than the velocity of a 1.0 MeV electron.¹⁷

Figure 4 shows the motion of the current front for the cases where the beam was injected into nitrogen at 40μ and hydrogen at 600μ . Also shown is the extrapolated trajectory of the ion bunch generated on each pulse, calculated from the arrival time at the first screen and the velocity as measured by TOF. The indication that the ion bunch was formed and accelerated well behind the current front was unambiguous in nearly all cases in hydrogen (150μ - 650μ) and nitrogen (35μ - 95μ).

Despite the wide spatial and temporal gap between the positive particle bunch and the beam current front, a striking agreement was found between the final proton velocity and the current front velocity as measured in the region $6.35 \text{ cm} \leq z \leq 16.5 \text{ cm}$. Figure 5 shows these data. (Corresponding current front velocity data for nitrogen was not taken. The current front velocity in $z < 16 \text{ cm}$ was generally different [usually found to be less] than the current front velocity in $z > 16 \text{ cm}$.) The

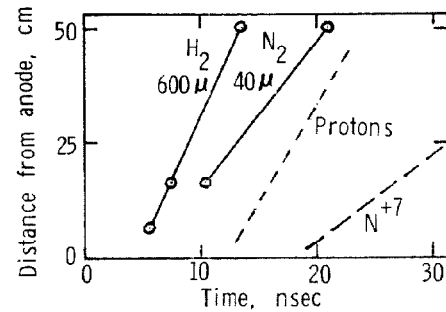


Fig. 4 Current front and corresponding ion bunch trajectory from two pulses.

velocity agreement shown in Figure 5 qualitatively confirms the measurements of Rander,⁵ whereas the present demonstration that the proton bunch was well behind the current front differs from his inference that the proton bunch coincides with the current front.

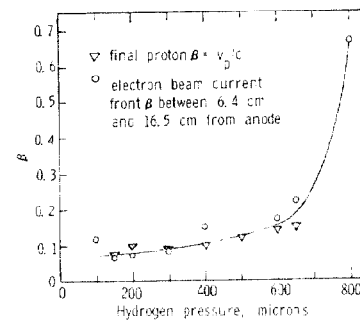


Fig. 5 Correlation between proton final velocity and velocity of electron beam current front.

Interpretation

In this section we briefly consider some of the possible acceleration cut-off mechanisms. The following interpretations of the data just presented are largely inferential and, therefore, not conclusive. They are offered mainly as a guide to further experimental and theoretical work.

The data given at the end of Section A under Results suggest possible reasons for the observed high-pressure cut-off of the acceleration process: (a) some of the protons "fall out" the rear end of the moving potential well that accelerates them. This gives the momentum spread, which increases as well velocity increases. At 800 μ the well velocity was high enough, in this view, that all protons fell behind before appreciable acceleration occurred. (b) It is the proton bunch formation process that was impaired as pressure increased: Ionization of background hydrogen during the bunch-formation phase has the effect of blurring or smearing the final bunch. At 800 μ the rate of ionization of hydrogen around the would-be proton bunch was sufficiently rapid to quench the formation of the bunch.

The power consumed by proton acceleration can be estimated using data presented above as the product of the total number of

accelerated protons, the final proton velocity, and the accelerating field strength. Taking representative experimental parameters, approximately 5×10^9 watts are required to sustain the proton bunch acceleration at 12 MeV, or about 10 percent of the peak beam power. Neglecting other beam energy losses, the beam power was evidently within an order of magnitude of being a limiting factor in our experiments.

The applied longitudinal magnetic field data supports the involvement of two-dimensional beam motion in the accelerating process, as postulated by LPM. Approximately a 6 kG field would be required to suppress beam pinching according to the criterion of De Packh.¹⁸ This estimate neglects beam induced changes in the longitudinal field as well as electric field effects. The strong effect of relatively small fields, 250 and 500 G, can be argued from beam paramagnetism, generated by radial contraction of the envelope as the beam enters a region of higher charge neutralization (e.g., the ion bunch). Paramagnetism, of course, limits the final pinch radius; an estimate of a minimum pinch radius can be obtained from conservation of canonical angular momentum, and by assuming that pinching proceeds with uniform field until all electron energy is rotational. This procedure gives ~ 0.85 cm as the minimum radius for the 500 G case. The pinch ratio in this estimate is still adequate to argue 10^5 - 10^6 V/cm accelerating fields, however. The observation that proton flux but not energy was affected by the small fields, taken together with the above remarks, indicates that the bunch formation phase, and not the acceleration phase, was affected by the small longitudinal magnetic fields. This inference in turn suggests that the proton acceleration was limited by a propagation velocity.

A velocity limitation in the case of proton acceleration is also suggested by the observation that the final proton velocity equalled beam front velocity, even though 50 centimeters typically separated the proton bunch from the beam front (Section E). The observation of increased proton energy with decreased beam temperature (Section A) indicates the same point. The critical ratio of background ion to beam electron charge densities required to prevent radial expansion of the beam envelope is lower for colder beams. Colder beams therefore have higher front velocities, and the data is consistent with these remarks. The electron beam used by Rander⁵ arrived at $Z=50$ cm at $t=37$ nsec (in 120 μ hydrogen), while our colder beam reached this same location at $t=20.3$ nsec (100 μ hydrogen) and $t=19.6$ nsec (150 μ hydrogen).

As described in Section C, we observed equal ion energy per charge (proton and N^{+7}) when several ion species were present with varying charge to mass ratios (protons and N^{+7}) in the experiments). Energy then appeared not to be velocity limited, but by accelerating field strength and/or length of the acceleration region. These features can be understood phenomenologically in the LPM picture as being due either to ion depletion and/or a very rapid sequence of bunch formations and accelerations, where average

charge-to-mass ratio decreases with successive bunches and where each new bunch consumes enough energy to cut off acceleration of the preceding bunch.

Only a brief treatment of the data and of our interpretation has been possible here. A more complete treatment is reserved for future publication. Nevertheless, even without detailed analyses these new data show conclusive evidence for 1 MeV/cm accelerating fields, acceleration to energies of tens of MeV, and large proton currents.

ACKNOWLEDGEMENTS: The authors are pleased to express their gratitude to the following people for their generous assistance: Dr. H. Heckman of the Lawrence Berkeley Laboratory for advice on emulsion analysis; A. Smith of the LBL Health Physics Department for the proton flux measurements using boron nitride; C. Parks of Physics International Company (PI) for congenially and efficiently handling the fabrication and operation of much of the apparatus; Dr. J. Benford and Dr. C. Stallings of PI for useful discussions on applied magnetic field effects; and N. Goldstein of PI for advice and help with various radiation diagnostics.

References

1. J. Rander, B. Ecker, G. Yonas, and D. Drickey, *Phys. Rev. Letters* **24**, 283 (1970).
2. S. Graybill and J. Uglum, *J. Appl. Phys.* **41**, 236 (1970).
3. S. Graybill, *IEEE Trans. Nuc. Sci.* NS-18, 3, 438 (1971).
4. S. Graybill, *IEEE Trans. Nuc. Sci.* NS-19, 2, 292 (1972).
5. J. Rander, *Phys. Rev. Letters* **25**, 13, 893 (1970).
6. J. Rander, J. Benford, B. Ecker, G. Loda, and G. Yonas, *Ion Acceleration Experiments with Intense Electron Beams*, PIIR-2-71, Physics International Company, San Leandro, CA., (1971); unpublished.
7. N. Rostoker, *Acceleration of Ions in Intense MeV Electron Beams*, VII International Conference on High Energy Acceleration, Yerevan, Armenia, USSR (1969).
8. A. A. Plyutto, et al., *Acceleration of Ions in an Electron Beam*, *Atomnaya Energiya*, **27**, 418 (1969).
9. B. Eastlund and J. Wachtel, *Bull. Amer. Phys. Soc.* **14**, 1047 (1969).
10. J. R. Uglum, S. E. Graybill and W. H. McNeil, *Bull. Amer. Phys. Soc.* **14**, 1047 (1969).
11. S. Putnam, *Phys. Rev. Letters* **25**, 1129 (1970).
12. S. Putnam, *IEEE Trans. Nuc. Sci.* NS-18, 496 (1971).
13. A. M. Sessler, *Comments in Nuclear Particle Physics* **3**, 93 (1969).
14. J. D. Lawson, *Particle Acc.* **3**, 21 (1972).
15. G. Yonas, *Symposium on Collective Methods of Acceleration*, Dubna, USSR (1972).
16. L. Bradley, T. Martin, and R. Parker, *Sandia Laboratories*, private communication.
17. S. Putnam, *Theoretical Studies of Intense Relativistic Beam-Plasma Interactions*, PIFR-72-105, Physics International Company, San Leandro, CA., (1972); unpublished.
18. D. C. De Packh, *Radiation Project Internal Report No. 7*, Naval Research Laboratory, Washington, D.C., April 1968.